

QCD effective charge and the structure function F_2 at small- x

E.G.S. Luna,¹ A.A. Natale,² and A.L. dos Santos¹

¹*Instituto de Física e Matemática, Universidade
Federal de Pelotas, 96010-900, Pelotas, RS, Brazil*

²*Instituto de Física Teórica, UNESP - Universidade Estadual Paulista,
Rua Dr. Bento T. Ferraz, 271, Bloco II,
01140-070, São Paulo - SP, Brazil*

Abstract

We study infrared contributions to the QCD description of the HERA data on the structure function F_2 within the *generalized* DAS approximation. We argue that this approximation is a natural one and consistent with the phenomenon of dynamical mass generation in QCD. The investigation is performed at next-to-leading order by using the leading-twist expansion of $F_2(x, Q^2)$ and by adopting an effective charge whose finite infrared behavior is constrained by a dynamical gluon mass. We propose one ansatz for the behavior of this effective coupling beyond leading order. The dependence of the experimental data on the infrared value of the effective charge is used in order to study the asymptotic behavior of the running gluon mass. The deep inelastic structure function F_2 obtained in this approach shows very good agreement with the experimental data.

I. INTRODUCTION

The nucleon structure function $F_2(x, Q^2)$ at low Q^2 has been measured in the previously unexplored small- x regime at the HERA collider. The deep-inelastic scattering of leptons off nucleons is the instrumental tool for high precision measurements of the quark and gluon content of the nucleons and the low Q^2 transition region bring us into a kinematical region where non-perturbative QCD effects becomes essential in order to understand the proton constitution. Despite the partonic splitting to be quite well understood through the use of the Dokshitzer-Gribov-Lipatov-Altarelli-Parisi (DGLAP) evolution equations [1], and these equations being known to describe the data even at not so large Q^2 , there is no reason to expect that they are reliable in the very small- x region. However, perturbative QCD effects are expected to become apparent at small- x , where gluon emission off the incoming parton leads to power series in $\alpha_s \ln(1/x)$. Resumming of this series via the Balitsky-Fadin-Kuraev-Lipatov (BFKL) equation [2], besides producing an $x^{-\lambda}$ behavior for the gluon distribution, generates its own characteristic Q^2 dependence. Hence approaching the low Q^2 transition region from the perturbative side makes evident the problem of how to incorporate in an effective way non-perturbative corrections into the evolution scenario.

Fortunately, this problem can be properly addressed by bringing up information about the infrared properties of QCD, more specifically, by considering the possibility that the non-perturbative dynamics of QCD generate an effective gluon mass at very slow Q^2 region. This dynamical gluon mass is intrinsically related to an infrared finite strong coupling constant [3], and its existence is strongly supported by recent QCD lattice simulations [4] as well as by phenomenological results [5–7]. It is opportune to remember that phenomenological infrared modifications of the strong-coupling constant are quite usual in the literature [8, 9], nevertheless the fact that an infrared finite coupling constant appears as a consequence of a dynamically generated gluon mass is much less known. Furthermore, the dynamical gluon mass that constrains the finite coupling constant turns up as the natural infrared cutoff in many perturbative QCD calculations, besides being responsible for a smooth transition from the perturbative to the non-perturbative QCD behavior [6, 7].

Our task of calculating infrared contributions to the QCD description of the HERA data on the deep-inelastic structure function, $F_2(x, Q^2)$, can succeed in a consistent way by analyzing exclusively the small- x region since, in this limit, some of the existing analytical

solutions of the DGLAP equation can be directly used [10–13]. Within this approach the HERA data at small- x is interpreted in terms of the double-asymptotic-scaling (DAS) phenomenon [10] related to the asymptotic behavior of the DGLAP equation in asymptotically free field theories [14]. The analytical solutions, valid in principle at very small- x and large- Q^2 values, can be extended in order to include the subasymptotic part of the Q^2 evolution, in what is called *generalized* DAS approximation [9, 15–17], leading to small- x asymptotic predictions for parton distribution functions evolved from flat x distributions at some starting point Q_0^2 for the DGLAP evolution. In particular, a recent analysis of F_2 and its derivatives $\partial F_2/\partial \ln Q^2$ and $\partial \ln F_2/\partial \ln(1/x)$ within this approach shows a good agreement with HERA data of deep-inelastic scattering for $Q^2 \gtrsim 1.5 \text{ GeV}^2$ [9].

One may wonder why the *generalized* DAS approximation works so beautifully in the small- x limit. This fact may be a signal that the choice of a flat distribution for the parton distribution function $f_a(x, Q^2)$ at some initial value Q_0^2 is quite appropriate for the DGLAP dynamics, more specifically [18],

$$f_a(x, Q_0^2) = A_a \quad (a = q, g) , \quad (1)$$

where A_a are unknown constants to be determined from the data, or in other way, that QCD predicts at small- x that $F_2(x, Q^2)$ should exhibit double scaling even at not so large- Q^2 values, provided only that the small- x behavior of the partonic distributions at some initial input Q_0^2 is sufficiently soft. Actually it was also pointed out that a flat gluon distribution in the small- Q^2 region appears naturally in QCD [7], within a model for hadronic cross section including the phenomenon of dynamical gluon mass generation, which naturally leads to a “frozen” infrared effective charge. This mechanism, based on first principles, is probably what is behind the good agreement of the *generalized* DAS approach with the experimental data.

Hence the purpose of this Letter is to compute the structure function $F_2(x, Q^2)$ of the proton by means of the *generalized* DAS approximation [9, 16, 17], assuming the flat initial parton distributions as a natural condition for QCD with dynamically generated gluon masses, and compare the results with the experimental data of $F_2(x, Q^2)$ in the infrared Q^2 region. In our calculations the non-perturbative dynamics of QCD is introduced by using the infrared finite QCD effective charge dependent on the dynamical gluon mass. As this effective strong-coupling has not been determined up to the next-to-leading order (NLO)

approximation, we propose one ansatz for its behavior at higher order.

The Letter is organized as follows: in the next section we introduce the *generalized* DAS approach beyond the leading order (LO), and discuss the underlying QCD dynamics behind the flat distribution and the frozen effective charge behaviors. In the Sec. III we propose an ansatz for the NLO behavior of the dynamical strong-coupling based on the property of multiplicative renormalizability, showing that this effective coupling reproduces the canonical NLO perturbative behavior at large Q^2 . Our results are presented in the Sec. IV, where the analysis of $F_2(x, Q^2)$ data is carried on using the formalism developed in the previous sections. In Sec. V we present our conclusions.

II. THE GENERALIZED DAS APPROXIMATION

The present data of $F_2(x, Q^2)$ imply a steep gluon at small- x , and there are some successful descriptions of F_2 by means of DGLAP evolution in the NLO approximation [19]. This steep behavior can be generated from a flat- x gluon distribution at some initial low Q_0^2 scale, or alternatively it can be directly included into the input distribution to be evolved from some higher scale. At sufficiently small- x we must resum the power series in $\alpha_s \ln(1/x)$ via BFKL equation. The result of this procedure is sensitive to the infrared k_T region and, for running α_s , it is found that

$$\tilde{g}(x, k_T^2) \sim C(k_T^2) x^{-\lambda}, \quad (2)$$

where $\lambda \sim 0.5$ [20]. Here $\tilde{g}(x, k_T^2)$ is the *unintegrated* gluon distribution and hence the resummation program requires knowledge of the gluon for all k_T^2 including the infrared region. However, in this confinement region the BFKL equation is not expected to be valid. Ultimately, with decreasing x , the singular behavior must be suppressed by non-perturbative effects.

The problem of calculating these infrared effects can be addressed by the so called QCD-based eikonal models [6, 21], which incorporate soft and semihard processes in the treatment of high energy hadron-hadron interactions. At high energies semihard processes are expected to give an increasing and significant part of the total hadronic cross sections [22]. Owing to the rapid growing of the number of semihard gluons in the hadron at fixed transverse momentum, the asymptotic behavior of these cross sections is determined chiefly by the gluon

distribution. In some QCD-based models these small- x semihard gluons play a central role, and a phenomenological “BFKL-inspired” gluon distribution is introduced [6, 7],

$$g(x, Q^2) = h(Q^2) x^{-J}, \quad (3)$$

which captures all the non-perturbative dynamics via the function $h(Q^2)$. Note that here $g(x, Q^2)$ is the traditional gluon distribution determined by the parton analysis of the $F_2(x, Q^2)$ data and whose Q^2 evolution is controlled by the DGLAP equations, where

$$\tilde{g}(x, k_T^2) = \left. \frac{\partial(xg(x, Q^2))}{\partial \ln Q^2} \right|_{Q^2=k_T^2}. \quad (4)$$

Recently it was shown that, in order to generate radiatively gluons at small- x , a rapid increase of $h(Q^2)$ with the momentum has to be accompanied by a fast increase of the J in such way that soft values of J are preferred at low Q^2 [7]. This picture is consistent with the statement that the steeply-rising gluon component is absent at low Q^2 and as Q^2 increases it is generated radiatively through perturbative evolution. In the Regge-exchange language the quantity J , that controls the asymptotic behavior of the total cross sections, is the universal “soft” Pomeron intercept, whose value has been phenomenologically determined to be $J = \alpha_{\mathbb{P}}(0) = 1 + \epsilon \sim 1.1$ [23, 24]. This is to be contrasted with the “hard” or “Lipatov” Pomeron intercept $\alpha_L(0) = 1 + \lambda \sim 1.5$. Therefore, fits to a set of hadronic data through QCD-based models show that J starts at a value where the gluon distribution is almost flat, $J(Q^2 \sim 0) \approx \alpha_{\mathbb{P}}(0)$, and as Q^2 increases the valence-like character of the gluon rapidly disappears [6, 7]. It is worth noting that these results are corroborated by a MRST analysis of parton distributions of proton [25]. From fitting the sea quark (S) and gluon (G) distributions of the default MRST partons to the forms $f_i(x, Q^2) = A(Q)x^{-\lambda_i(Q^2)}$ as $x \rightarrow 0$, $i = S, G$, they have observed that as Q^2 increases from the input scale $Q_0^2 = 1 \text{ GeV}^2$ the flat behavior of the gluon rapidly disappears due to evolution being driven by the much steeper sea. For higher values of Q^2 the gluon exponent λ_G increases rapidly and becomes higher than the sea quark exponent λ_S , since the gluon drives the sea quark via the $g \rightarrow \bar{q}q$ transition. More specifically, λ_G starts at a value $\lambda_G \approx 0$ at $Q^2 \approx 1 \text{ GeV}^2$, and by $Q^2 \approx 4 \text{ GeV}^2$ it has the value $\lambda_G = 0.2$. Hence a flat input gluon distribution at low momenta, that appears as the natural condition for QCD evolution with dynamically generated gluon masses, also comes out in standard perturbative procedures.

In the *generalized* DAS approach [9, 15–17] the subasymptotic corrections are included via the finite parts of anomalous dimensions of Wilson operators and Wilson coefficients.

Remember that in the *standard* DAS approximation only the singular parts of the anomalous dimensions are taken into account. In the *generalized* approach the flat input gluon distribution (1) determines the small- x asymptotics and, at NLO, the twist-two (leading) term of $F_2(x, Q^2)$ is given by [15–17]

$$F_2(x, Q^2) = e \left[f_q(x, Q^2) + \frac{4T_R n_f}{3} \frac{\alpha_s(Q^2)}{4\pi} f_g(x, Q^2) \right], \quad (5)$$

where $e = \sum_i^f e_i^2/n_f$ is the average charge squared of the effective number n_f of quarks, $T_R = 1/2$ is the color factor for $g \rightarrow q\bar{q}$ splitting, and

$$f_a(x, Q^2) = f_a^+(x, Q^2) + f_a^-(x, Q^2) \quad (a = q, g); \quad (6)$$

the “+” and “−” representation above follows from the solution, at leading twist approximation, of the DGLAP equation in the Mellin moment space [16]:

$$f_a^-(x, Q^2) = A_a^-(Q^2, Q_0^2) \exp[-d_-(1)s - D_-(1)p] + \mathcal{O}(x), \quad (7)$$

$$f_g^+(x, Q^2) = A_g^+(Q^2, Q_0^2) \tilde{I}_0(\sigma) \exp[-\bar{d}_+(1)s - \bar{D}_+(1)p] + \mathcal{O}(\rho), \quad (8)$$

$$\begin{aligned} f_q^+(x, Q^2) &= A_q^+(Q^2, Q_0^2) \left[\left(1 - \bar{d}_{+-}^q(1) \frac{\alpha_s(Q^2)}{4\pi} \right) \rho \tilde{I}_1(\sigma) + \frac{20C_A}{3} \frac{\alpha_s(Q^2)}{4\pi} \tilde{I}_0(\sigma) \right] \\ &\times \exp[-\bar{d}_+(1)s - \bar{D}_+(1)p] + \mathcal{O}(\rho), \end{aligned} \quad (9)$$

where $s = \ln[\alpha_s(Q_0^2)/\alpha_s(Q^2)]$, $p = [\alpha_s(Q_0^2) - \alpha_s(Q^2)]/4\pi$, $D_\pm(n) = d_{\pm\pm}(n) - (\beta_1/\beta_0)d_\pm(n)$, $\sigma = 2\sqrt{(\hat{d}_+s + \hat{D}_+p) \ln x}$ and $\rho = \sqrt{(\hat{d}_+s + \hat{D}_+p) / \ln x} = \sigma/2 \ln(1/x)$; here β_0 (β_1) is the first (second) coefficient of the QCD β function, \tilde{I}_ν ($\nu = 0, 1$) are functions related to the modified Bessel function I_ν , and the components of the anomalous dimension $d_-(n)$ as well as of the singular (\hat{d}) and regular (\bar{d}) parts of $d_+(n) = \hat{d}_+/(n-1) + \bar{d}_+(n)$, for $n \rightarrow 1$, are

$$\hat{d}_+ = -\frac{4C_A}{\beta_0}, \quad \bar{d}_+(1) = 1 + \frac{4n_f}{3\beta_0} \left(1 - \frac{C_A}{C_F} \right), \quad d_-(1) = \frac{4C_F n_f}{3C_A \beta_0}; \quad (10)$$

finally, the factors $A_a^{+,-}$ and the components of the singular and regular parts of the remaining anomalous dimensions D_\pm are given by

$$\begin{aligned} A_g^+(Q^2, Q_0^2) &= \left[1 - \bar{d}_{+-}^g(1) \frac{\alpha_s(Q^2)}{4\pi} \right] A_g \\ &+ \frac{C_F}{C_A} \left[1 - d_{-+}^g(1) \frac{\alpha_s(Q_0^2)}{4\pi} - \bar{d}_{+-}^g(1) \frac{\alpha_s(Q^2)}{4\pi} \right] A_q, \end{aligned} \quad (11)$$

$$A_g^-(Q^2, Q_0^2) = A_g - A_g^+(Q^2, Q_0^2), \quad (12)$$

$$A_q^+(Q^2, Q_0^2) = \frac{n_f}{3C_A} \left(A_g + \frac{C_F}{C_A} A_q \right), \quad (13)$$

$$A_q^-(Q^2, Q_0^2) = A_q - \frac{20C_A}{3} \frac{\alpha_s(Q_0^2)}{4\pi} A_q^+(Q^2, Q_0^2), \quad (14)$$

$$\hat{d}_{+++} = \frac{4n_f}{9\beta_0} (23C_A - 26C_F), \quad \hat{d}_{+-}^q = -\frac{20C_A}{3}, \quad \hat{d}_{+-}^g = 0, \quad (15)$$

$$\begin{aligned} \bar{d}_{++}(1) = & \frac{8}{3\beta_0} \left[\frac{C_A^2}{3} \left(36\zeta(3) + 33\zeta(2) - \frac{1643}{12} \right) \right. \\ & - \left(2C_F\zeta(2) + \frac{43}{9} C_A - \frac{547}{36} C_F + \frac{3C_F^2}{2C_A} \right) n_f \\ & \left. - \frac{13C_F}{18C_A} \left(1 - 2\frac{C_F}{C_A} \right) n_f^2 \right], \end{aligned} \quad (16)$$

$$\begin{aligned} d_{--}(1) = & \frac{4C_A C_F}{\beta_0} \left(1 - 2\frac{C_F}{C_A} \right) \left(2\zeta(3) - 3\zeta(2) + \frac{13}{4} + \frac{13}{27} \frac{n_f^2}{C_A^2} \right) \\ & + \frac{4C_F}{3\beta_0} \left(4\zeta(2) - \frac{47}{18} + 3\frac{C_F}{C_A} \right) n_f, \end{aligned} \quad (17)$$

$$\bar{d}_{+-}^q(1) = C_A \left(9 - 3\frac{C_F}{C_A} - 4\zeta(2) \right) - \frac{13}{9} \left(1 - 2\frac{C_F}{C_A} \right) n_f, \quad (18)$$

$$\bar{d}_{+-}^g(1) = \frac{20n_f C_F}{9 C_A}, \quad d_{-+}^q(1) = 0, \quad d_{-+}^g(1) = - \left[C_A + \frac{1}{3} \left(1 - 2\frac{C_F}{C_A} \right) n_f \right] \quad (19)$$

where $C_A = N$, $C_F = (N^2 - 1)/2N$, and ζ is the Riemann zeta function. From now on we set $N = 3$ in order to fix the Casimir color-factors $C_A (= 3)$ and $C_F (= 4/3)$. With all these definitions we can discuss in the next section the QCD effective charge that we shall use in our calculation.

III. THE QCD EFFECTIVE CHARGE AT NLO

Although not extensively known in phenomenological studies, there is increasing evidence that QCD develops an effective, momentum-dependent mass for the gluons, while preserving the local $SU(3)_c$ invariance of the theory. Of course this mass is not a bare one and at

few GeV its signal is already erased from the physical amplitudes, which merge into the perturbative QCD calculations. In this scenario there is a natural scale that, in principle, introduces a threshold for gluons to pop up from the vacuum [26].

Since the gluon mass generation is a purely dynamical effect, the formal tool for tackling this non-perturbative problem, in the continuum, is provided by the Schwinger-Dyson equations [27]. These equations constitute an infinite set of coupled non-linear integral equations governing the dynamics of all QCD Green's functions. In particular, within this framework the generation of a dynamical gluon mass is associated with the existence of infrared finite solutions for the gluon propagator $\Delta_{\mu\nu}(q^2)$ [28–30]. In covariant gauges, the gluon propagator has the form

$$\Delta_{\mu\nu}(q^2) = -i \left[P_{\mu\nu}(q) \Delta(q^2) + \xi \frac{q_\mu q_\nu}{q^4} \right], \quad (20)$$

where ξ is the gauge-fixing parameter and $P_{\mu\nu}(q) = g_{\mu\nu} - q_\mu q_\nu / q^2$. Infrared finite solutions ($\Delta^{-1}(0) > 0$) can be fit by massive propagators on the form $\Delta^{-1}(q^2) = q^2 + m^2(q^2)$, where $m^2(q^2)$, which depends non-trivially on the momentum transfer q^2 , is the so called dynamical gluon mass. If the renormalization-group logarithms are included in the Schwinger-Dyson analysis, the non-perturbative generalization of the QCD running coupling, the effective charge $\bar{\alpha}_s(q^2)$, is obtained [28, 29].

Recent studies of a non-linear Schwinger-Dyson equation for the gluon self-energy show that $m^2(Q^2)$ may in fact have two distinct asymptotic behaviors [31] (note that from now on we adopt the virtuality Q in our calculations); first, the dynamical gluon mass runs as an inverse power of a logarithm; second, $m^2(Q^2)$ drops as an inverse power of momentum. The logarithmic running of $m^2(Q^2)$ has been found in previous studies of linearized Schwinger-Dyson equations to behave as $m^2(Q^2) \sim (\ln Q^2)^{-1-\gamma}$, with $\gamma > 1$ [28, 32]. In the non-linear case [31] this behavior is rewritten as

$$m^2(Q^2) = m_g^2 \left[\frac{\ln \left(\frac{Q^2 + \rho m_g^2}{\Lambda^2} \right)}{\ln \left(\frac{\rho m_g^2}{\Lambda^2} \right)} \right]^{-1-\gamma_1}, \quad (21)$$

where $\gamma_1 = -6(1 + c_2 - c_1)/5$; here c_1 and c_2 are parameters of the ansatz for the (fully dressed) three-gluon vertex used in the numerical analysis of the gluon self-energy. Their values are restricted by a “mass condition” which controls the behavior of the dynamical mass in the ultraviolet region. In the case of a logarithmic running, $c_1 \in [0.15, 0.4]$ and

$c_2 \in [-1.07, -0.92]$ [31]; the values of the parameters ρ and m_g , which control the behavior of $m^2(Q^2)$ in the infrared region, are also restricted by the mass condition, and general constraints are satisfied for $\rho \in [1.0, 8.0]$ and $m_g \in [300, 800]$ MeV [33]. It is worth mentioning that the dynamical gluon mass was found for the first time by Cornwall to be equal to [28]

$$m^2(Q^2) = m_g^2 \left[\frac{\ln \left(\frac{Q^2 + 4m_g^2}{\Lambda^2} \right)}{\ln \left(\frac{4m_g^2}{\Lambda^2} \right)} \right]^{-\frac{12}{11}}, \quad (22)$$

where the infrared mass value m_g is phenomenologically determined and typically of the order $m_g = 500 \pm 200$ MeV [5–7, 28, 34]. Note that the Cornwall expression (22) is a special case of the logarithmic running mass (21); more specifically, (22) can be obtained from (21) by fixing $\rho = 4$ and $\gamma_1 = 1/11$.

A power-law running behavior for $m^2(Q^2)$ was first envisaged in [28, 35]. According to an OPE calculation the most probable asymptotic behavior of the running gluon mass is proportional to $1/Q^2$ [36]. At the level of a non-linear Schwinger-Dyson equation this asymptotic behavior is given by

$$m^2(Q^2) = \frac{m_g^4}{Q^2 + m_g^2} \left[\frac{\ln \left(\frac{Q^2 + \rho m_g^2}{\Lambda^2} \right)}{\ln \left(\frac{\rho m_g^2}{\Lambda^2} \right)} \right]^{\gamma_2 - 1}, \quad (23)$$

where $\gamma_2 = (4 + 6c_1)/5$; for power law running the mass condition imposes $c_1 \in [0.7, 1.3]$; the ρ and m_g parameters are constrained to lie in the same interval as before, namely $\rho \in [1.0, 8.0]$ and $m_g \in [300, 800]$ MeV [31, 33].

The results of Ref.[31] are precise with respect to the gross asymptotic behavior of the running gluon mass which are represented by our equations (21) and (23). Eq.(5.2) of that reference contains a broad definition of the mass function used to match the numerical results, and it must be said that the approximations in there exclude the ghost fields and the regularization of quadratic divergences is obtained through what is called ‘‘tadpole-condition’’. This procedure does not determine $\bar{\alpha}_s(0)$ and m_g univocally, and leads to a dispersion on the frozen coupling infrared behavior. However, this uncertainty is systematically reduced by the aforementioned phenomenological studies [5–7], which determine a frozen value for the LO effective charge of the order $\bar{\alpha}_s(0) \sim 0.7 \pm 0.2$. Our result for the NLO frozen behavior, $\bar{\alpha}_s^{NLO}(0) \sim 0.6$, despite not being directly comparable to LO results, gives support to the statement that the dynamical gluon mass m_g is not strongly dependent

on the perturbation order. Moreover, our value $\bar{\alpha}_s^{NLO}(0) \sim 0.6$ is totally consistent with the frozen value $\alpha_s(0)/\pi \sim 0.19$, obtained very recently from an analytic QCD model [37].

Given the running behavior of $m^2(Q^2)$, the leading-order QCD effective charge $\bar{\alpha}_s(Q^2)$ is written as

$$\bar{\alpha}_s(Q^2) = \frac{1}{b_0 \ln \left(\frac{Q^2 + 4m^2(Q^2)}{\Lambda^2} \right)}, \quad (24)$$

where $b_0 = \beta_0/4\pi = (1/4\pi)[(11C_A - 2n_f)/3]$ and $\Lambda \equiv \Lambda_{QCD}^{LO}$. The effective charge clearly shows the existence of an infrared fixed point as $Q^2 \rightarrow 0$, i.e., the dynamical mass term tames the Landau pole and $\bar{\alpha}_s$ freezes at a finite value in the infrared limit. It must be stressed that the fixed point does not depend on a specific process, it is uniquely obtained as we fix Λ and, in principle, it should be exactly determined if we knew how to solve QCD. Note that in the limit $Q^2 \gg \Lambda^2$ the dynamical mass $m(Q^2)$ vanishes, and the effective charge (24) matches with the one-loop perturbative QCD coupling $\alpha_s(Q^2)$. It means that the asymptotic ultraviolet behavior of the LO running coupling, obtained from the renormalization group equation perturbation theory,

$$\alpha_s^{LO}(Q^2 \gg \Lambda^2) \sim \frac{1}{b_0 \ln \left(\frac{Q^2}{\Lambda^2} \right)}, \quad (25)$$

is reproduced in solutions of Schwinger-Dyson equations, provided only that the truncation method employed in the analysis preserves the multiplicative renormalizability (MR). Since the MR is an important feature of gauge field theories, and holds for any renormalization scale, we argue that a QCD effective charge at NLO, $\bar{\alpha}_s^{NLO}$, can be successfully built by saturating the two-loop perturbative strong coupling α_s^{NLO} , that is, by introducing the replacement $\alpha_s^{NLO}(Q^2) \rightarrow \bar{\alpha}_s^{NLO}(Q^2) = \alpha_s^{NLO}(Q^2 + 4m^2(Q^2))$ into the perturbative result. In this way, the QCD effective charge at NLO is given by

$$\bar{\alpha}_s^{NLO}(Q^2) = \frac{1}{b_0 \ln \left(\frac{Q^2 + 4m^2(Q^2)}{\Lambda^2} \right)} \left[1 - \frac{b_1 \ln \left(\ln \left(\frac{Q^2 + 4m^2(Q^2)}{\Lambda^2} \right) \right)}{b_0^2 \ln \left(\frac{Q^2 + 4m^2(Q^2)}{\Lambda^2} \right)} \right], \quad (26)$$

where $b_1 = \beta_1/16\pi^2 = (1/16\pi^2)[(34C_A^2 - n_f(10C_A + 6C_F))/3]$ and $\Lambda = \Lambda_{QCD}^{NLO}$. Note that in the limit $Q^2 \gg \Lambda^2$ the effective charge (26) matches with the canonical two-loop perturbative coupling, α_s^{NLO} , in such a way that the relation

$$\frac{\bar{\alpha}_s^{NLO}}{\bar{\alpha}_s^{LO}} = \frac{\alpha_s^{NLO}}{\alpha_s^{LO}} \quad (27)$$

is valid in the ultraviolet region. This relation is expected to be valid if the Schwinger-Dyson equation is renormalized multiplicatively.

We have created other ansatzes preserving the relation (27), where an intermediate scale was introduced in order to separate the perturbative and non-perturbative regions, but they did not introduce significant differences in the behavior of $\bar{\alpha}_s^{NLO}$ in the infrared region. Thus we have adopted the coupling (26) as the standard ansatz in our calculations of the structure function $F_2(x, Q^2)$ of the proton. We do not expect that any phenomenological calculation using the logarithmic and power-law running dynamical masses will be strongly dependent on the asymptotic behavior as they are on the infrared one. Therefore, since the calculation is quite dependent on the behavior of the effective charge in the infrared region, and our analysis includes HERA data sets at low and moderate Q^2 , we carry out two independent global fits to HERA data: in the first one we adopt the effective charge (26) with a logarithmic mass running, expression (21); in the second fit the effective charge runs through the power-law mass running, expression (23). Within this procedure we can investigate if the experimental data can differentiate these solutions. The different momentum behaviors of the canonical (perturbative) and the effective charges are shown in Fig.1.

IV. RESULTS

From the formalism discussed in the previous sections, we analyze $F_2(x, Q^2)$ data sets at low and moderate Q^2 values [38], by adding the statistic and systematic errors in quadrature. We carry out global fits to F_2 data by means of a χ^2 fitting procedure with an interval $\chi^2 - \chi_{min}^2$ corresponding to the projection of the χ^2 hypersurface containing 90% of probability. To keep the analysis as simple as possible, we fix $n_f = 4$ and $\Lambda = 284$ GeV. These choices are not only consistent to NLO procedures, but are also the same ones adopted in Ref. [9]. Concerning the QCD effective charges, we fix in all the fits $\rho = 4$, since this is the optimal value obtained by Cornwall in order to reproduce the numerical results of a gauge invariant Schwinger-Dyson equation for the gluon propagator [28]. Moreover, we observe that the gluon mass scale m_g is not very sensitive to ρ (at least in this leading-twist operator analysis), changing by about 12% (4%) when ρ ranges from 1.0 to 8.0 in the case of a logarithmic (power-law) running behavior.

Our first analysis consisted in the determination of the A_g , A_q and Q_0^2 values from a global

fit to F_2 data using the canonical (perturbative) QCD coupling at NLO. The χ^2/DoF for this fit was 2.88. These values are shown in Table I, and the structure functions corresponding to these values are shown by the dotted-dashed curves in Fig.2. It is clear from the relatively high value of χ^2/DoF obtained in this fit, as well as from the curves depicted in Fig.2, that the canonical version of the coupling constant provides a worse fit for the x dependence of $F_2(x, Q^2)$ for specific Q^2 bins, and the disagreement is larger for smaller values of Q^2 . This result was expected in the light of an earlier analysis on F_2 data, which showed the requirement for theoretical improvements in the QCD canonical coupling for smaller Q^2 values [9]. More specifically, it was shown that modifications in the strong coupling based on the Källén-Lehmann Q^2 analyticity [39], or on a purely phenomenological freezing, improve the description of the experimental F_2 data at low Q^2 . Our results for $F_2(x, Q^2)$ in the case of the standard perturbative coupling are therefore similar to the ones of Ref.[9]. It is important to stress that the analytic coupling constant used in the Ref.[9] has a frozen value $\alpha_s(0) \simeq 1.398$, which is not consistent with phenomenological results using the gluon dynamical mass. Moreover, this analytic coupling, as pointed out by Cvetič, Kögerler and Valenzuela [37], does not give the correct value of the well-measured semihadronic τ decay ratio r_τ , namely $r_\tau^{exp} = 0.203 \pm 0.004$. However, the analytic coupling version of the Ref.[37], besides generating a frozen value similar to the one obtained in this Letter, reproduces successfully the experimental value of r_τ .

In the second analysis we carried out a global fit to F_2 data using the QCD effective charge with a logarithmic running mass, namely, using the expressions (21) and (26). In principle, the infrared mass scale m_g and the factor γ_1 are also, together with A_g , A_q and Q_0^2 , fitting parameters to be determined, where the constraints on c_1 and c_2 are satisfied for $\gamma_1 \in [0.084, 0.564]$. However, the best χ^2 value for this fit is obtained at $\gamma_1 = 0.084$. If we carry out global fits to different combinations of F_2 data sets, as for example taking into account only data sets with $Q^2 < 2.0 \text{ GeV}^2$ or $Q^2 \geq 2.0$, we observe that the optimum χ^2 for each fit has all $\gamma_1 = 0.084$. Therefore, we have set $\gamma_1 = 0.084$ in our subsequent analysis. The χ^2/DoF obtained by this fit was 1.87. The values of m_g , A_g , A_q and Q_0^2 are show in the second line of the Table I. The structure functions corresponding to these values are shown by the solid curves in Fig.2.

In the sequence we have obtained m_g , A_g , A_q and Q_0^2 by means of a fit to F_2 data using the QCD effective charge with a power-law running mass, namely, using the expressions

(23) and (26). In this analysis γ_2 , constrained by c_2 to lie in the interval $[1.64, 2.36]$, is set to $\gamma_2 = 2.36$, since the optimum χ^2 for fits to different combinations of data is obtained for $\gamma_2 = 2.36$. The χ^2/Dof for this global fit was 2.13. The values of m_g , A_g , A_q and Q_0^2 are show in the third line of the Table I. The theoretical F_2 results corresponding to these values are shown by the dashed curves in Fig.2.

Note that all Q_0^2 dependence enters into the α_s definition. In our approach Q_0^2 will always appear added to a factor $4m^2(Q_0^2)$. Particularly in the case of log-running gluon mass the Q_0^2 dependence is not felt strongly, as a consequence of a very flat infrared coupling constant. In this case the “effective” initial scale $Q_{eff,0}^2$ is dominated by the term $4m^2(Q_0^2)$, namely $Q_{eff,0}^2 = 0.009 + 4m^2(0.009) \approx 0.534 \text{ GeV}^2$. On the other hand a power-law running gluon mass leads to a α_s behavior that matches very fast with the standard perturbative one and consequently a stronger dependence on the Q_0^2 parameter, where $Q_{eff,0}^2 = 0.029 + 4m^2(0.029) \approx 0.456 \text{ GeV}^2$. These values are close to the result from Ref.[9] for the NLO fit using a frozen coupling, namely $Q_0^2 = 0.589 \pm 0.006 \text{ GeV}^2$.

It seems that owing to the larger χ^2/Dof value obtained in the power-law mass analysis the data favors the logarithmic running mass case, but it must be said that the differences are quite subtle and in both cases we have a substantial improvement in the agreement of the theory with the experimental HERA data at low Q^2 .

V. CONCLUSIONS

In this Letter we have computed the structure function $F_2(x, Q^2)$ of the proton by means of the *generalized* DAS approximation with a QCD effective charge at NLO. This effective strong coupling is finite in the infrared region and naturally connected to the phenomenon of dynamical gluon mass generation in QCD. Its basically flat behavior below the m_g scale indicates the existence of an infrared fixed point.

We have observed that an infrared finite coupling constant is fundamental in order to improve the description of the $F_2(x, Q^2)$ experimental data at low Q^2 , what can easily be seen if we compare the results using effective charges with the one using the canonical perturbative coupling. Such fact was already observed in Ref.[9], in which a phenomenological infrared finite coupling was also adopted. We stress that our QCD effective charges, despite the same freezing behavior of the couplings adopted in [9], are obtained from the QCD Lagrangian,

i.e., they are derived from first principles, in a scenario where infrared effects are taken into account. Moreover, we have argued that a flat x initial condition in the DGLAP evolution equations, which determine the basic role of the singular parts of the anomalous dimensions in the generalized DAS approach, is naturally related to what is expected from non-perturbative QCD, i.e., from QCD with dynamically generated gluon masses.

Through global fits to F_2 data we have obtained the best values of the infrared mass scale in the case of the logarithmic and power-law running mass, $m_g = 364 \pm 26$ MeV and $m_g = 355 \pm 27$ MeV, respectively. It is important noting that these infrared scale values are of the same order of magnitude as the values obtained in other calculations of strongly interacting processes [5–7]. These results corroborate theoretical analyzes considering the generation of a dynamical gluon mass in non-perturbative QCD.

Our results show that the leading-twist approximation of the Wilson operator product expansion is quite accurate on the description of the structure function F_2 data. However, our results using QCD effective charges indicates that, at principle, in order to differentiate the logarithmic running mass from the power-law one, a higher-twist study is necessary. An analysis using higher twist corrections to the expansion of $F_2(x, Q^2)$ is in progress.

ACKNOWLEDGMENTS

We are grateful to A.C. Aguilar, V.P. Gonçalves and W.K. Sauter for valuable discussions. This research was partially supported by the Conselho Nacional de Desenvolvimento Científico e Tecnológico (CNPq) and by the Coordenação de Aperfeiçoamento de Pessoal de Nível Superior (CAPES).

-
- [1] V.N. Gribov, L.N. Lipatov, Sov. J. Nucl. Phys. 15 (1972) 438 [Yad. Fiz. 15 (1972) 781]; L.N. Lipatov, Sov. J. Nucl. Phys. 20 (1975) 94 [Yad. Fiz. 20 (1974) 181]; G. Altarelli, G. Parisi, Nucl. Phys. B 126 (1977) 298; Yu.L. Dokshitzer, Sov. Phys. JETP 46 (1977) 641 [Zh. Eksp. Teor. Fiz. 73 (1977) 1216].
 - [2] L.N. Lipatov, Sov. J. Nucl. Phys. 23 (1976) 338; V.S. Fadin, E.A. Kuraev, L.N. Lipatov, Sov. Phys. JETP 44 (1976) 443; V.S. Fadin, E.A. Kuraev, L.N. Lipatov, Sov. Phys. JETP 45 (1977) 199; Y.Y. Balitsky, L.N. Lipatov, Sov. J. Nucl. Phys. 28 (1978) 822.

- [3] A. C. Aguilar, A. A. Natale, P. S. Rodrigues da Silva, *Phys. Rev. Lett.* 90 (2003) 152001.
- [4] F.D.R. Bonnet, et al., *Phys. Rev. D* 64 (2001) 034501; A. Cucchieri, T. Mendes, A. Taurines, *Phys. Rev. D* 67 (2003) 091502(R); P.O. Bowman, et al., *Phys. Rev. D* 70 (2004) 034509; A. Sternbeck, E.-M. Ilgenfritz, M. Muller-Preussker, A. Schiller, *Phys. Rev. D* 72 (2005) 014507; A. Sternbeck, E.-M. Ilgenfritz, M. Muller-Preussker, *Phys. Rev. D* 73 (2006) 014502; Ph. Boucaud, et al., *JHEP* 0606 (2006) 001; P.O. Bowman, et al., hep-lat/0703022; I.L. Bogolubsky, E.M. Ilgenfritz, M. Muller-Preussker, A. Sternbeck, *Phys. Lett* 676 (2009) 69; O. Oliveira, P. J. Silva, arXiv:0910.2897 [hep-lat]; O. Oliveira, P. J. Silva, arXiv:0911.1643 [hep-lat]; A. Cucchieri, T. Mendes, E.M.S. Santos, *Phys. Rev. Lett.* 103 (209) 141602; A. Cucchieri, T. Mendes, *Phys. Rev. D* 81 (2010) 016005; D. Dudal, O. Oliveira, N. Vandersickel, *Phys. Rev. D* 81 (2010) 074505.
- [5] F. Halzen, G. Krein, A.A. Natale, *Phys. Rev. D* 47 (1993) 295; M.B. Gay Ducati, F. Halzen, A.A. Natale, *Phys. Rev. D* 48 (1993) 2324; A.C. Aguilar, A. Mihara, A.A. Natale, *Phys. Rev. D* 65 (2002) 054011; M.B. Gay Ducati, W.K. Sauter, *Phys. Lett. B* 521 (2001) 259; M.B. Gay Ducati, W.K. Sauter, *Phys. Rev. D* 67 (2003) 014014; E.G.S. Luna, *Phys. Lett. B* 641 (2006) 171; E.G.S. Luna, A.A. Natale, *Phys. Rev. D* 73 (2006) 074019; E.G.S. Luna, *Braz. J. Phys.* 37 (2007) 84; E.G.S. Luna, in: *AIP Conference Proceedings*, vol. 1296, American Institute of Physics, New York, 2010, p. 183; E.G.S. Luna, A.L. dos Santos, in: *AIP Conference Proceedings*, vol. 1296, American Institute of Physics, New York, 2010, p. 330.
- [6] E.G.S. Luna, A.F. Martini, M.J. Menon, A. Mihara, A.A. Natale, *Phys. Rev. D* 72 (2005) 034019.
- [7] E.G.S. Luna, A.A. Natale, C.M. Zanetti, *Int. J. Mod. Phys. A* 23 (2008) 151.
- [8] E. Eichten, et al., *Phys. Rev. Lett.* 34 (1975) 369; E. Eichten, et al., *Phys. Rev. D* 21 (1980) 203; J.L. Richardson, *Phys. Lett. B* 82 (1979) 272; G. Parisi, R. Petronzio, *Phys. Lett. B* 94 (1980) 51; T. Barnes, F. E. Close, S. Monaghan, *Nucl. Phys. B* 198 (1982) 380; S. Godfrey, N. Isgur, *Phys. Rev. D* 32 (1985) 189; A.C. Mattingly, P. M. Stevenson, *Phys. Rev. Lett.* 69 (1992) 1320; A.C. Mattingly, P. M. Stevenson, *Phys. Rev. D* 49 (1994) 437; Yu.L. Dokshitzer, B.R. Webber, *Phys. Lett. B* 352 (1995) 451; Yu.L. Dokshitzer, G. Marchesini, B.R. Webber, *Nucl. Phys. B* 469 (1996) 93; M. Anselmino, F. Murgia, *Phys. Rev. D* 53 (1996) 5314; B. Badelek, J. Kwiecinsky, A. Stasto, *Z. Phys. C* 74 (1997) 297; A. Mihara, A.A. Natale, *Phys. Lett. B* 482 (2000) 378.

- [9] G. Cvetič, A.Y. Illarionov, B.A. Kniehl, A.V. Kotikov, Phys. Lett. B 679 (2009) 350.
- [10] R.D. Ball, S. Forte, Phys. Lett. B 336 (1994) 77; R.D. Ball, S. Forte, Acta Phys. Polon. B 26 (1995) 2097; R.D. Ball, S. Forte, Nucl. Phys. B (Proc. Suppl.) 54A (1997) 163.
- [11] G.M. Frichter, D.W. McKay, J.P. Ralston, Phys. Rev. Lett. 74 (1995) 1508.
- [12] C. López, F. Barreiro, F.J. Ynduráin, Z. Phys. C 72 (1996) 561; K. Adel, F. Barreiro, F.J. Ynduráin, Nucl. Phys. B 495 (1997) 221.
- [13] A.V. Kotikov, Mod. Phys. Lett. A 11 (1996) 103; A.V. Kotikov, Phys. Atom. Nucl. 59 (1996) 2137 [Yad. Fiz. 59 (1996) 2219].
- [14] A. De Rújula, S.L. Glashow, H.D. Politzer, S.B. Treiman, F. Wilczek, A. Zee, Phys. Rev. D 10 (1974) 1649.
- [15] L. Mankiewicz, A. Saalfeld, T. Weigl, Phys. Lett. B 393 (1997) 175.
- [16] A.V. Kotikov, G. Parente, Nucl. Phys. B 549 (1999) 242.
- [17] A.Y. Illarionov, A. V. Kotikov, G. Parente Bermudez, Phys. Part. Nucl. 39 (2008) 307.
- [18] Note that in the expression (1) the parton distributions $f_a(x, Q_0^2)$ are multiplied by x , namely, $f_g(x, Q^2) \equiv xg(x, Q^2)$, $f_q(x, Q^2) \equiv xq(x, Q^2)$.
- [19] A.M. Cooper-Sarkar, R.C.E. Devenish, A. de Roeck, Int. J. Mod. Phys. A 13 (1998) 3385; J. Breitweg, et al., Eur. Phys. J. C 7 (1999) 609; C. Adloff, et al., Eur. Phys. J. C 13 (2000) 609.
- [20] A.J. Askew, J. Kwiecinski, A.D. Martin, P.J. Sutton, Phys. Rev. D 47 (1993) 3775; A.J. Askew, J. Kwiecinski, A.D. Martin, P.J. Sutton, Phys. Rev. D 49 (1994) 4402.
- [21] R.M. Godbole, A. Grau, G. Pancheri, Y.N. Srivastava, arXiv:1001.4749.
- [22] L.V. Gribov, E.M. Levin, M.G. Ryskin, Phys. Rep. 100 (1983) 1; E.M. Levin, M.G. Ryskin, Phys. Rep. 189 (1990) 267.
- [23] A. Donnachie, P.V. Landshoff, Phys. Lett. B 296 (1992) 227; R.J.M. Covelan, J. Montanha, K. Goulianos, Phys. Lett. B 389 (1996) 176; J.R. Cudell, K. Kang, S.K. Kim, Phys. Lett. B 395 (1997) 311; E.G.S. Luna, M.J. Menon, Phys. Lett. B 565 (2003) 123; R.F. Avila, E.G.S. Luna, M.J. Menon, Phys. Rev. D 67 (2003) 054020; E.G.S. Luna, M.J. Menon, J. Montanha, Nucl. Phys. A 745 (2004) 104; E.G.S. Luna, M.J. Menon, J. Montanha, Braz. J. Phys. 34 (2004) 268.
- [24] E.G.S. Luna, V.A. Khoze, A.D. Martin, M.G. Ryskin, Eur. Phys. J. C 59 (2009) 1; E.G.S. Luna, V.A. Khoze, A.D. Martin, M.G. Ryskin, Eur. Phys. J. C 69 (2010) 95.
- [25] A.D. Martin, R.G. Roberts, W.J. Stirling, R.S. Thorne, Eur. Phys. J. C 4 (1998) 463.

- [26] J.M. Cornwall, A. Soni, Phys. Lett. B 120 (1983) 431; J.M. Cornwall, A. Soni, Phys. Rev. D 29 (1984) 1424.
- [27] F.J. Dyson, Phys. Rev. 75 (1949) 1736; J.S. Schwinger, Proc. Nat. Acad. Sci. 37 (1951) 452.
- [28] J.M. Cornwall, Phys. Rev. D 26 (1982) 1453.
- [29] J.M. Cornwall, J. Papavassiliou, Phys. Rev. D 40 (1989) 3474; J. Papavassiliou, J.M. Cornwall, Phys. Rev. D 44 (1991) 1285.
- [30] D. Binosi, J. Papavassiliou, JHEP 0811 (2008) 063; D. Binosi, J. Papavassiliou, Phys. Rept. 479 (2009) 1; A.C. Aguilar, J. Papavassiliou, Phys. Rev. D 81 (2010) 034003.
- [31] A.C. Aguilar, J. Papavassiliou, Eur. Phys. J. A 35 (2008) 189.
- [32] A.C. Aguilar, J. Papavassiliou, JHEP 0612 (2006) 012.
- [33] A.C. Aguilar, private communication, 2010.
- [34] A.A. Natale, PoS (QCD-TNT 09) 031 (2009); arXiv:0910.5689.
- [35] J.M. Cornwall, W.S. Hou, Phys. Rev. D 34 (1986) 585.
- [36] M. Lavelle, Phys. Rev. D 44 (1991) 26; D. Dudal, J.A. Gracey, S.P. Sorella, N. Vandersickel, H. Verschelde, Phys. Rev. D 78 (2008) 065047.
- [37] G. Cvetič, R. Kögerler, C. Valenzuela, Phys. Rev. D 82 (2010) 114004.
- [38] I. Abt, et al., Nucl. Phys. B 407 (1993) 515; T. Ahmed, et al., Nucl. Phys. B 439 (1995) 471; M. Derrick, et al., Z. Phys. C 65 (1995) 379; M. Derrick, et al., Z. Phys. C 69 (1996) 607; M. Derrick, et al., Z. Phys. C 72 (1996) 399; S. Aid, et al., Nucl. Phys. B 470 (1996) 3; C. Adloff, et al., Nucl. Phys. B 497 (1997) 3; J. Breitweg, et al., Phys. Lett. B 407 (1997) 432; J. Breitweg, et al., Eur. Phys. J. C 7 (1999) 609; J. Breitweg, et al., Phys. Lett. B 487 (2000) 53; C. Adloff, et al., Eur. Phys. J. C 21 (2001) 33; S. Chekanov, et al., Eur. Phys. J. C 21 (2001) 443.
- [39] D.V. Shirkov, I.L. Solovtsov, Phys. Rev. Lett. 79 (1997) 1209.

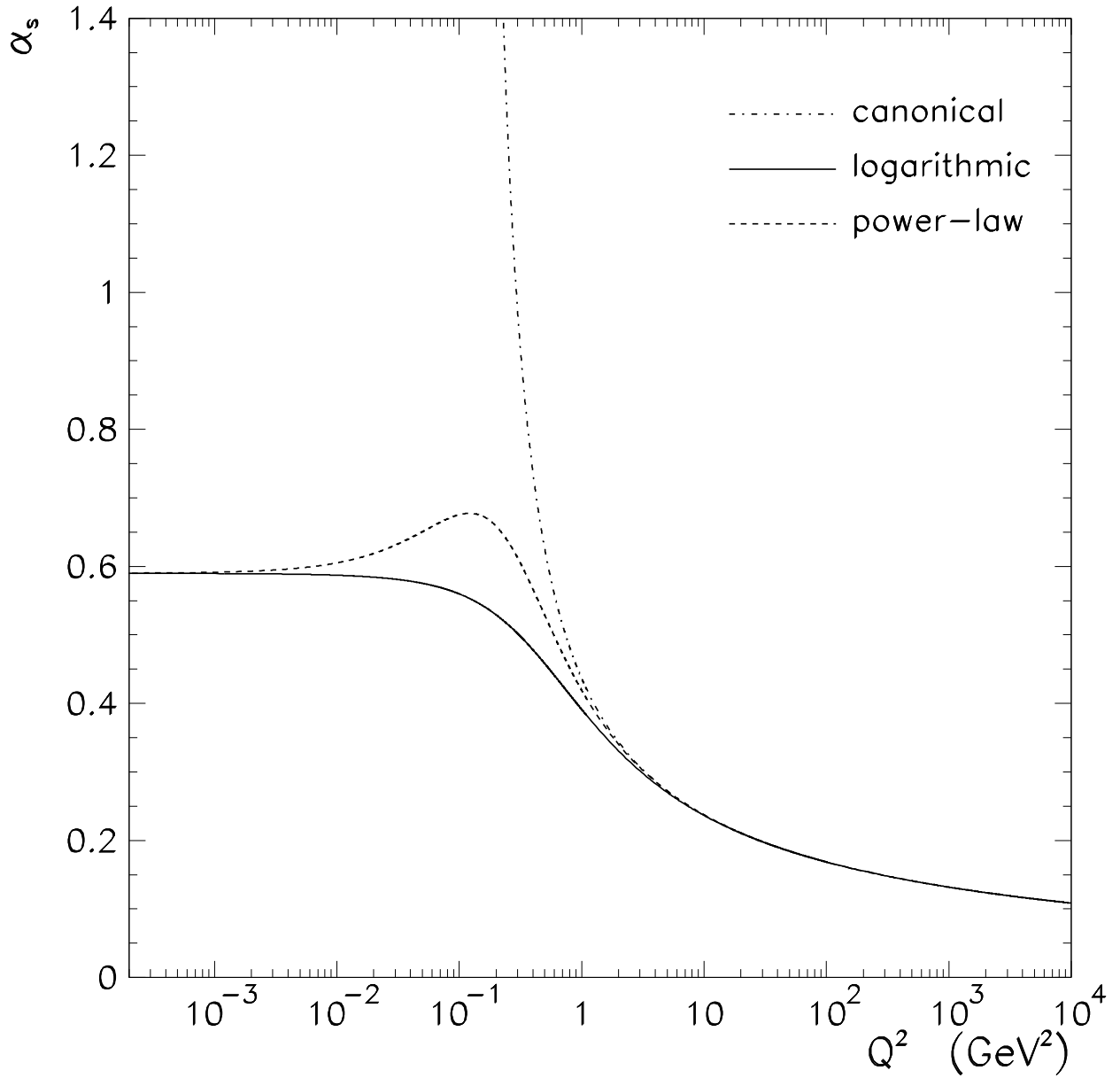


FIG. 1. The canonical (perturbative) coupling constant and the QCD effective charge with logarithmic and power-law mass running at NLO.

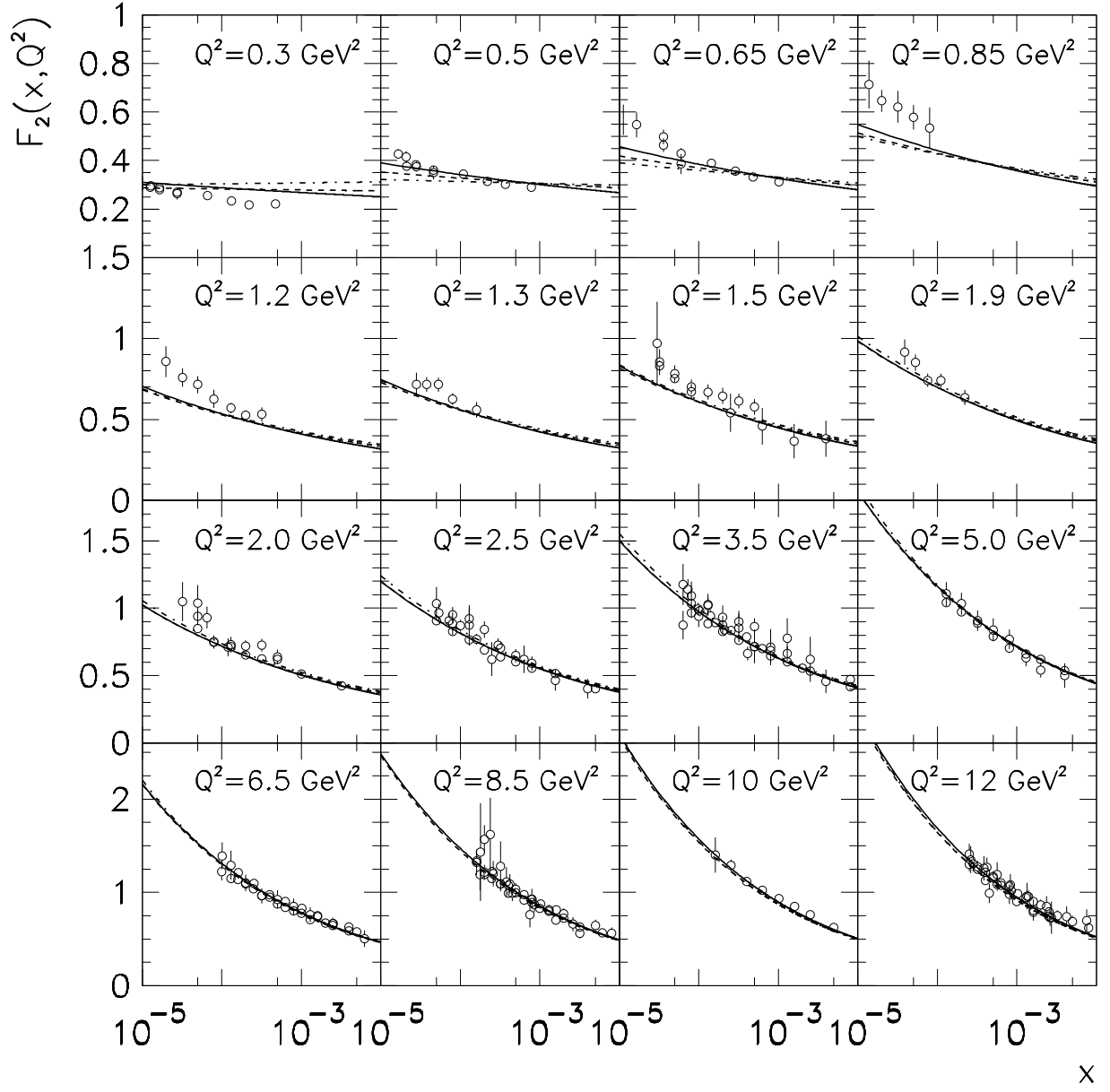


FIG. 2. Fits of the x dependence of $F_2(x, Q^2)$ for specific Q^2 with the QCD effective charge dependent on a dynamical gluon mass. The solid curves were obtained considering the logarithmic running gluon mass, Eq.(21), whereas the dashed curves correspond to the power-law running case, Eq.(23). The dotted-dashed curves correspond to the perturbative behavior at NLO.

Coupling	m_g [MeV]	A_g	A_q	Q_0^2 [GeV ²]	χ^2/DoF
Canonical	-	-0.339 ± 0.019	1.119 ± 0.025	0.414 ± 0.016	2.88
Logarithmic	364 ± 26	-0.084 ± 0.063	0.843 ± 0.069	0.009 ± 0.116	1.87
Power-Law	355 ± 27	-0.253 ± 0.041	1.018 ± 0.565	0.029 ± 0.008	2.13

TABLE I. Values of the parameters m_g , A_g , A_q and Q_0^2 resulting from the global fit to F_2 data. The errors were obtained assuming a confidence region of the parameters of 90%.